

Lasers in Manufacturing Conference 2017

Surface oxidation of titanium by cw-Nd:YAG laser

A. Rodríguez^{*}, J.N. Montero, J.M. Amado, M.J. Tobar, A. Yáñez

Universidade da Coruña, Dpto. Ingeniería Industrial II, Ferrol, E-115403, Spain

Abstract

Titanium oxide coatings present interesting properties, as high chemical stability, biocompatibility, very good adhesion and excellent mechanical properties, which makes them very attractive for several applications, as medical implants or tools used in corrosive and aggressive environments. Moreover, due to the generation of the oxide layer, the surface is colored, which makes the coatings useful for decorative applications.

One of the techniques that can be used to achieve the oxidation of titanium is the laser oxidation treatment. The properties and color of the oxide layers obtained will depend on the laser beam parameters and those of the environment.

In this work surface oxidation of Titanium was performed by means of a Nd:YAG laser ($\lambda = 1064$ nm) in continuous wave mode under air environment. The effect of the process parameters on the oxide color and on the layer thickness growth was studied. A three dimensional heat FEM model coupled with an oxidation kinetics law was used to predict the oxide growth and the resultant color. The experimental and the numerical results obtained were compared in order to verify the model.

Keywords: Surface treatment; Laser oxidation; Titanium; Numerical simulation.

1. Introduction

Titanium and its alloys have a large number of applications in a wide range of industries, from pigments to aerospace or medical applications, Leyens. C and Peters. M, 2003. In particular if titanium surfaces are exposed to air they form an oxide passive layer which has interesting properties for biomedical applications,

^{*} Corresponding author. Tel.: +34-981-337-400.
E-mail address: angel.rcarballo@udc.es .

as it improves corrosion resistance and enhances osseous integration in body implants. Since the surfaces are colored due to the presence of the oxide layer they can also be used for decorative purposes.

Various oxidation methods exist as anodization, chemical treatments or thermal oxidation. Laser oxidation is a type of thermal oxidation which has some advantages as being a simple technique, having high processing speeds and being a highly localized and flexible technique.

Usually, laser oxidation is performed with pulsed lasers by accumulating pulses on the sample surface, Antonczak, A.J. et al.; Jwad, T., 2016. In this work laser oxidation has been performed in CP Ti with a Nd:YAG continuous wave laser by processing the surface line by line. Also a numerical model capable of predicting the resultant oxide thickness and color under certain process parameters has been developed. The results of the simulations have been compared with the experimental results.

2. Experimental setup

The laser metal deposition system is composed of a continuous wave diode pumped Nd:YAG laser (Rofin DY022) with a maximum power of 2200 W. Laser is sent through a fiber to the focusing optics system installed in a ABB IRB2400 six axis robot arm. A custom application controls and monitors all the steps of the process. Programming commands are transmitted via ftp and loaded into the ABB motion controller. Once loaded, the controller takes upon the movement of the robot according to the programmed speed and trajectory. It also sends the required voltage signals for switching on the laser and sets the required laser power level during the process.

In this work CP Ti samples have been oxidized in air with a Nd:YAG laser in continuous wave mode. The areas scanned were irradiated using parallel lines. The samples have been smoothed with sandpaper and cleaned before processing. The parameters need to be chosen carefully in order to avoid the possible melting due to overheating on the zone directly located under the center of the laser beam, circumstance not desirable for an oxidation treatment. Different process parameters: laser power, laser scan velocity, spot diameter and distance between lines have been tested to obtain different oxidation results.

3. Numerical model

When a metal exposed to air is heated by a laser beam, an oxide layer grows on the surface of the material. The growth of the oxide layer depends on the thermal cycle experimented by the points near the surface which is being irradiated. Therefore, to estimate the oxide growth is necessary to obtain the thermal field on the material at each time.

The numerical simulation presented in this work consists of three consecutive steps which are carried out for each time step along the duration of the laser treatment. First the temperature of the substrate is calculated, then the temperature field is used for the calculation of the oxide thickness and from the thickness values the color of the oxide can be determined at every point.

3.1. Thermal model

The temperature of the material during the laser processing is modeled by the three dimensional heat equation:

$$\frac{\partial(\rho(T)c(T)T)}{\partial t} - \nabla * (k(T)\nabla T) = Q(t) \quad \text{in } \Omega \quad (1)$$

Subject to the boundary conditions:

$$T(x, t) = T_{boundary}(x, t)$$

$$k(T) \frac{\partial T}{\partial n} = -h(T - T_{\infty}) + q''$$

And initial conditions

$$T(x, 0) = T_0(x)$$

where T is the temperature (K), ρ the density (kg/m³), c the specific heat (J/K), k the thermal conductivity (W/(m K)), Q the volumetric heat generation (W/m³), h the film convection coefficient (W/(m²K)) and q'' the heat flux (W/m²).

The heat equation is numerically solved by the finite element method using the deal.II library, Bangerth, W. et al., 2007. The sample under irradiation is discretized in elements and the resultant system of equations is solved to obtain the nodal temperatures. The thermal properties of the material are considered to be dependent on the temperature; this makes the heat equation nonlinear and a Newton scheme is needed to solve it.

During the process, the laser beam provides the energy necessary to heat the substrate. For the simulation the beam is modeled as a moving gaussian flux acting on the surface of the substrate. The irradiance of the laser beam is given by:

$$I = \frac{2P}{\pi w^2} e^{-\frac{2r^2}{w^2}} \left(\frac{W}{m^2} \right) \quad (2)$$

where P is the laser power (W), w the radius at which the irradiance drops to 1/e² of the maximum value (m) and r the radial distance to the center of the beam (m). The elements hit by the laser beam are automatically computed with a ray tracing algorithm and the heat flux is applied to the faces of the elements. The laser power is partially absorbed by the material through its absorption coefficient, which depends on the material, the characteristics of the surface and the temperature. When a layer of oxide is formed, the absorption of laser light is enhanced; therefore the absorption needs to be increased on the areas where a previous oxide layer exists. In the laser oxidation process there is no melting of the material, thus there is not melt pool fluid movement to be accounted for and the heat equation should model the temperature field quite well.

3.2. Oxide thickness model

Once the thermal field is computed the oxide growth can be calculated. The present model considers that the oxide growth follows a parabolic law, Kofstad. P et al., 1958:

$$\frac{dy}{dt} = \frac{k}{y} \quad (3)$$

where y is the thickness of the oxide layer and k the parabolic rate constant. The kinetic constant k obeys the Arrhenius equation and it has the form:

$$k = k_0 * e^{-\frac{Q}{RT}} \quad (4)$$

where k_0 is the oxidation constant, Q (J) the activation energy of the oxidation reaction, R (J/(K mol)) the universal gas constant and T (K) the absolute temperature. The constants of the oxidation reaction k_0 and Q can be calculated experimentally using gravimetric analysis. In this work the oxidation constants are calculated from the gravimetric curves in Takayama, I., 1994. As seen in the equation (4) the kinetic constant depends on the temperature, thus the equation (3) can be integrated at each time step once the temperature field has been solved. Substituting equation (4) in equation (3) and integrating the resultant equation on a time step $[t_0, t_1]$ gives:

$$\frac{dy}{dt} = \frac{k}{y} = \frac{k_0 * e^{\frac{-Q}{RT(t)}}}{y}$$

$$\int_{y_0}^{y_1} y dy = \int_{t_0}^{t_1} k_0 e^{\frac{-Q}{RT(t)}} dt$$

$$\Delta y^2 = 2k_0 \int_{t_0}^{t_1} e^{\frac{-Q}{RT(t)}} dt \quad (5)$$

The solution of equation (5) gives the oxide growth in the time step. In order to simplify the integral of the right hand side, the temperature curve is assumed to have a linear profile within the time step, which is a plausible hypothesis if the time step is small. Using this simplification and rearranging the equation:

$$\Delta y^2 = 2k_0 \int_{t_0}^{t_1} e^{\frac{-Q}{R(T_0 + \frac{t-t_0}{t_1-t_0}(T_1-T_0))}} dt = 2k_0 \int_{t_0}^{t_1} e^{\frac{-Q}{at+b}} dt \quad (6)$$

where T_0 and T_1 are the temperatures at the beginning and at the end of the time step and the constants a and b are given by:

$$a = R \frac{T_1 - T_0}{t_1 - t_0} \quad b = R \left[T_0 - \frac{t_0(T_1 - T_0)}{t_1 - t_0} \right]$$

Finally, the solution of the equation (6) is:

$$\Delta y^2 = 2k_0 \frac{Q Ei\left(-\frac{Q}{b+at}\right) + (at+b)e^{-\frac{Q}{at+b}}}{a} \Bigg|_{t_0}^{t_1} \quad (7)$$

where Ei is the exponential integral. The equation (7) is evaluated at every node of the surface of the FEM model to obtain the oxide growth at those positions for the current time step. A fine mesh is needed to resolve the oxide, therefore an adaptive mesh refinement technique, as shown in the Fig. 1, has been used to refine the elements only in the oxidized area, which helps to reduce the computational burden.

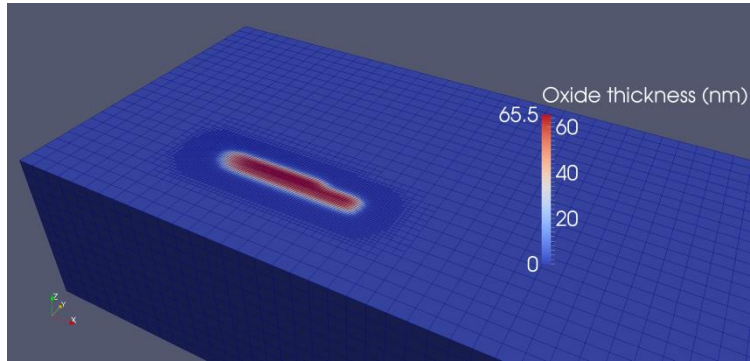


Fig. 1. Mesh used in a simulation and oxide thickness calculation.

3.3. Oxide color calculation

The colors seen on a titanium oxidized surface are caused by light interference taking place at the metal-oxide-air interfaces. Therefore the resultant color of the oxide depends on the thickness of the oxide film and on the refractive index of the mediums (air, oxide and titanium), Diamanti, M. V, et al. 2008. For the calculations the oxide layer is supposed to be almost entirely composed by TiO₂. Under an illuminant D65, which roughly resembles the average midday light, and using an angle of incidence to the surface of 60°, the resultant colors relative to the oxide film thickness are shown in Fig. 2 .

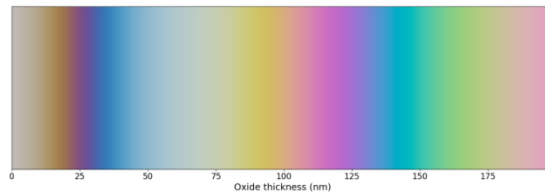


Fig. 2. Oxide color as function of oxide thickness.

4. Results

The oxide thickness depends on the thermal cycle experimented by the surface of the piece. By using a continuous wave laser the thermal process is much less localized than with a pulsed laser, which makes more difficult to achieve a homogeneous color across the treated surface.

In order to achieve a small heat affected zone a laser spot diameter of $w = 0.5$ mm has been used. To get a uniform oxide color the substrate can't overheat, as seen in the Fig. 3 (a), so the thermal cycle obtained in each laser individual scan should be similar, without producing a global rise in temperature. To accomplish this goal a high laser beam scanning speed of $v=300$ mm/s and a low laser power of $P = 210$ W have been chosen. The power could be further lowered but it is already close to the minimum power of the laser system used.

In this work, the distance between successive laser scans has been modified to obtain oxides of different colors, instead of changing the power and the scanning speed of the laser. As color changes are produced by

small variations in the oxide thickness of few nanometers, is difficult to find the right combinations of power and scanning speed with a continuous wave industrial laser which would yield the full color palette of the titanium oxide. If a pair of laser power and scanning speed is fixed and under the hypothesis that for those values the thermal field is the same for every line, increasing or decreasing the distance between lines will cause displacements in the color bar of Fig. 2. Thus, once a suitable power and speed pair is chosen, the other colors of the palette are easily obtained using this method.

This method is applied using the process parameters of Table 1 over six zones of a titanium plate of dimensions 15 x 15 x 3 mm. The distance between lines is set constant for each irradiated block, and is varied between 100 μm and 50 μm using decrements of 10 μm from the leftmost to the rightmost block. The results are shown in Fig. 3 (b).

Table 1. Process parameters

Process parameters	
Laser power (W)	210
v (mm/s)	300
Spot diameter (mm)	0.5
Distance between lines (μm)	100 - 50

If we compare the colors obtained in the sample with the color bar of the Fig. 2, it can be seen that we are sweeping the 30 – 125 μm thickness range. This is the range usually used when the titanium is colored because the colors correspondents to thicker layers, i.e. to the right on the color bar, tend to be less monochromatic. As the distance between lines is decreased, i.e. to the right on the Fig. 3 (b), the accumulated laser fluence on the surface is higher and thicker oxide layers are obtained, with the colors moving to the right of the color bar. Simulations have been carried out replicating the process parameters of the experiments shown below. The lines have been made shorter to reduce the simulation times, but this doesn't affect the results. The results are shown in Fig. 4. As it can be seen the simulated colors reproduce quite well the experimental results.

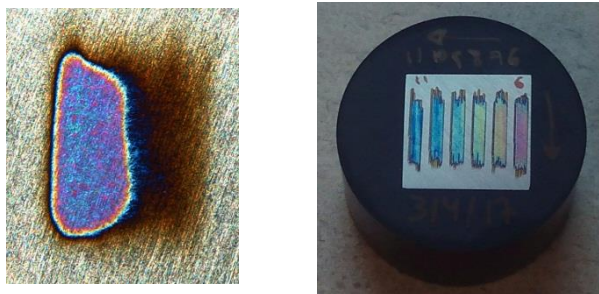


Fig. 3. (a) Inhomogeneous oxidized sample. (b) Sample of titanium irradiated. From left to right in order of decreasing distance between laser scans: 100 μm , 90 μm , 80 μm , 70 μm , 60 μm , 50 μm .

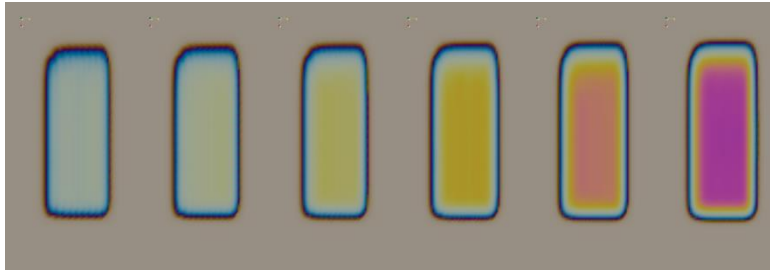


Fig. 4. Colors of areas oxidized calculated from the simulations. From left to right in order of decreasing distance between laser scans: 100 μm , 90 μm , 80 μm , 70 μm , 60 μm , 50 μm

In the Fig.5 microscope images of the samples are shown. In these images lines of two alternating colors can be clearly distinguished, which are blended by the eye when the image is not magnified. The presence of this pattern can be due two causes. On the one hand, when the division between the diameters of the laser spot and the distance between lines is not exact the laser doesn't irradiate the same number of times the entire surface. On the other hand due to the fact that the laser absorption is not the same in the Titanium that in the oxide, the energy absorbed through the layer is not uniform, which could also be responsible for the presence of alternating colors lines.

Changing the overlapping between laser scans produces different irradiance patterns, which in turn outputs different pairs of alternating colors. In Fig. 6 the color intensities along a line perpendicular to the beam scans are plotted for the samples of Fig. 3 (b). As it can be seen in the plots, the periods of the curves are coincident with the distance between adjacent laser lines. When the distance between lines is reduced the difference between the colors of consecutive lines gets smaller, an effect that can be appreciated in the intensity color profiles of the smallest distances, where the peaks and valleys are not clearly distinguishable.

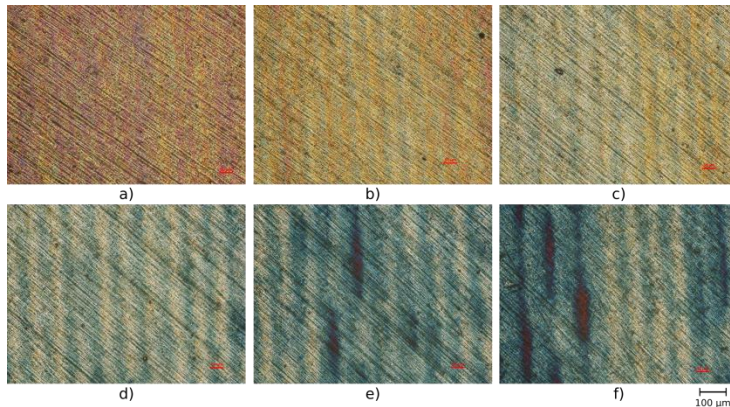


Fig. 5. Microscope images of the irradiated sample. The distance between laser lines are: (a) 50 μm ; (b) 60 μm ; (c) 70 μm ; (d) 80 μm , (e) 90 μm ; (f) 100 μm .

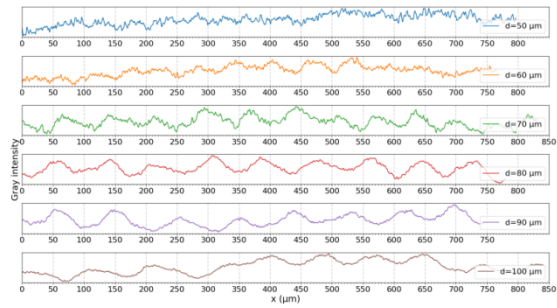


Fig. 6. Gray intensity profiles of the irradiated blocks.

The presence of alternating colors can be explained better looking at the graphs of the Fig. 7, where a series of consecutive beams (colored curves), each one representing the transversal irradiance of a beam scan, are shown. It is observed that each beam consists of a zone of high irradiance, which corresponds to the zone in which the preceding laser scans have created oxide and a zone of low irradiance in which the laser beam interacts with the pure titanium of the substrate.

The black line represents the summation of the irradiances of all the beams. When the oxide diameter is equal to the laser spot diameter, the difference in laser absorption doesn't affect the total irradiance. Otherwise, there is a gap between beginnings and ends of irradiance zones, whose total summation is not constant. The pattern can also be seen in the simulations if the mesh used is fine enough to resolve the overlapping displacement between lines. This is shown in the Fig. 8, where a simulation with distance between lines of $d=150 \mu\text{m}$ has been carried out. The layer is composed of lines of high and low fluence, similar to the effect seen in the microscope images.

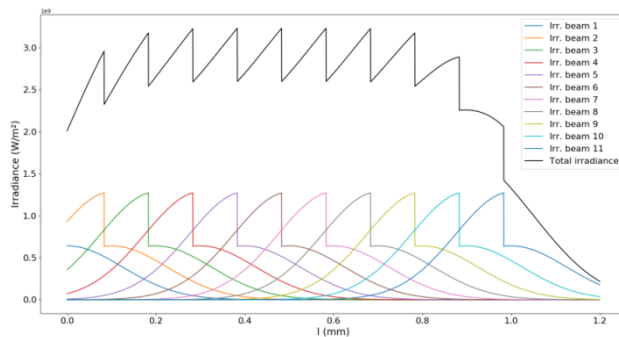


Fig. 7. Laser irradiance pattern.

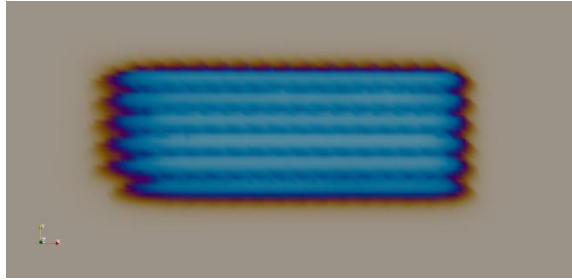


Fig. 8. Simulation with bands of alternating colors.

5. Conclusions

In this work CP Ti has been oxidized with a cw-Nd:YAG laser. Different colors have been obtained modifying the distance between parallel consecutive scans, and thus changing the mean energy deposited over the surface. A numerical model has been developed to simulate the laser oxidation process, using a finite element method to resolve the thermal field and the oxide thickness and color on the substrate. The colors obtained in the simulations closely resemble the ones obtained in the experiments.

The microscope images of the oxidized surfaces show a pattern of pairs of alternating colors. This pattern can be explained by a difference of the laser light absorption between the titanium and the oxide and by an inhomogeneous number of laser scans along the surface for some cases. This is consistent with the calculated fluence patterns and with fine simulations of the process.

Further study may establish continuous wave lasers as a viable alternative to the use of pulsed lasers for the oxidation of metallic parts.

References

- Antonczak, A. J., Stepak, B., Koziol, P. E., Abramski, K. M, 2014, The influence of process parameters on the laser induced coloring of titanium, *Applied Physics A* 115, p. 1003
- Bangerth, W., Hartmann, R., Kanschä, G., deal.II – a general-purpose object-oriented finite element library, 2007, *ACM Transactions on Mathematical Software* 33, no. 4, article 24
- Diamanti, M. V, Del Curto, B., Pedferri M., Interference colors of thin oxide layers on titanium, *Color research and application* 33, i. 3, p. 221
- Jwad, T., Deng, S., Butt, H., Dimov, S., 2016, Laser induced single spot oxidation of titanium, *Applied Surface Science* 387, p. 617
- Kofstad, P., Hauffe, K., Kjöllesdal, H., 1958, Investigation on the Oxidation Mechanism of Titanium, *Acta Chemica Scandinavica* 12, p. 239
- Leyens, C., Peters., M, 2003, *Titanium and Titanium Alloys: Fundamental and Applications*. Wiley-VCH, Germany
- Takayama I., 1994, *Development of Oxidation Protective Coating for Titanium*, Nippon Steel Technical Report 62, p. 57